Spectroscopic properties of neodymium-doped tellurite glass fiber

Junjie Zhang (张军杰), Shixun Dai (戴世勋), Guonian Wang (汪国年), Shiqing Xu (徐时清), Liyan Zhang (张丽艳), and Lili Hu (胡丽丽)

Shanghai Institute of Optics and Fine Mechanics, Chinese Academy of Science, Shanghai 201800

Received March 15, 2004

Nd^{3+}-doped tellurite glass and a single mode tellurite glass fiber with a core diameter of 8 μm were prepared in this work. The 1.33-μm emission from the $^4F_{3/2} \rightarrow {}^4I_{13/2}$ transition of Nd^{3+} with a spectral bandwidth of 55 nm in tellurite glass fiber is observed. The lifetime of 164 μs of $^4F_{3/2}$ level and quantum efficiency of about 100 % are obtained.

OCIS codes: 160.5690, 160.4670, 300.6280, 160.2750, 160.3130.

To obtain 1.3-μm emission, which has an important impact on telecommunications, mass-works have been done and remarkable progress has been made, mainly in Pr^{3+}- or Nd^{3+}-doped fluoride glass amplifiers[1−3]. $^4F_{3/2} \rightarrow {}^4I_{13/2}$ transition of Nd^{3+} has several important characteristics favoring efficient amplification in the 1.3-μm spectral region, and a lot of studies explored this possibility[3−5]. It is well know, however, that the spectroscopic properties of rare earth ions in glass are strongly affected by host glass compositions[6], because silica glass has serious drawback such as small-stimulated emission cross section, low limit of dopant level, and high fluorescence quenching, it is not suited to be the media for Nd^{3+} doping. So does the single mode Nd:crystalline laser for its low slope efficiency. Fluoride glasses are easily attacked by water and the precursor must be kept under a nitrogen atmosphere, so it is difficult to be used in fabricate integrated optical fluoride glass devices.

Tellurite glasses possess large transparency window ($0.35 - 6$ μm), high refractive index, good glass stability, and high rare earth ions solubility, and are attractive for developing infrared fiber lasers and amplifiers[6−9]. In this paper, we report our progress in a Nd^{3+}-doped tellurite glass fiber 1.3-μm optical amplifications.

Glasses with the composition of $75TeO_2$+$15ZnO$ +$5Na_2O$+$5Li_2O$ were prepared. The mixture of power was melt in Pt crucible at $800 - 850$°C for 10 minutes. The melt was cast into a preheated brass mold and then the obtained glasses were annealed at their glass transition temperatures determined by differential thermal analysis (DTA). Glass samples were cut and polished to the size of 10×10×1 mm for the spectrum measurements.

Core and cladding glasses were prepared by using the similar melting procedure as describing above for bulk glass. The core glass was doped with 1wt.-% Nd_2O_3. The preform was fabricated by the suction casting technology[10]. During the fiber drawing procedure, the fiber was coated with a low-refractive-index (n = 1.52) polymer (DSM DeSolite@3471-2-136) outer cladding to prevent mechanical fracture. An optical microscope equipped with a JVC CCD camera measured the core and cladding diameters of the fabricated fibers. The resulting fiber had a core diameter of ~ 20 μm and numerical aperture (NA) of 0.2. The average background loss was measured using the cutback method, and the value was 1.8 dB/m at 1310 nm.

The absorption spectrum of the bulk glass was measured by a PERKIN-ELMER-LANBDA 900UV/VIS/NIR spectrophotometer. An 800-nm, 2-W diode laser was used as pumping source.

The fluorescence spectra were measured with a JOBIN-YVON TRIAX550 fluorescence spectrometer. The beam of the pumping laser is coupled into the fiber using a precise positioning stage (M-561D, Newport). A mechanical chopper was used to modulate the pump, the fluorescence was detected using a fast response InGaAs detector, and the fluorescence decay curves were recorded using a Tektronix TDS3052 oscilloscope.

The room-temperature absorption spectrum of Nd^{3+}-doped tellurite glass was shown in Fig. 1. Transitions in the near infrared and the visible were easily assigned. Higher energy absorption bands largely overlap, resulting in a loss of accuracy. The spectra of the other host glasses are similar to these in Fig. 1, the only significant differences are small changes in the relative band intensities [11,12]. Most of the energy levels could be determined and the energy diagram of Nd^{3+} was shown in Fig. 2.

The Judd-Ofelt (J-O) theory is often applied to determine the important spectroscopic and laser parameters of rare-earth-doped glasses or crystals[13,14]. By employing a least squares fitting of the measured spectral absorbency according to the J-O model, the characteristic

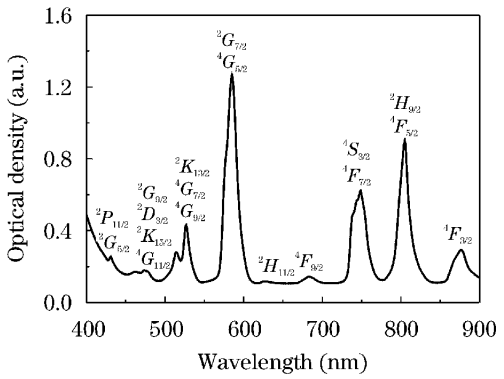

Fig. 1. Absorption spectrum of Nd^{3+}-doped tellurite glass.

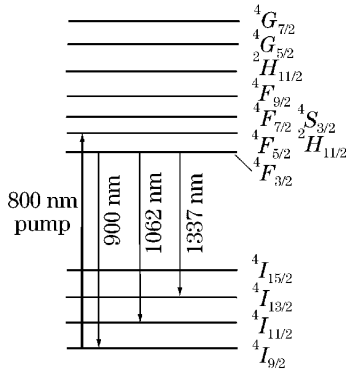

Fig. 2. Schematic diagram of energy levels of Nd^{3+}.

intensity parameters were determined. The J-O parameters $\Omega_t(t = 2, 4, 6)$ for the Nd^{3+}-doped tellurite glass are found to be $\Omega_2 = 3.78\times10^{-20}$, $\Omega_4 = 4.56\times10^{-20}$, and $\Omega_6 = 4.73\times10^{-20}$ cm^2. These values are closer to the values reported by Weber[11] and Pellegrino[12] *et al.*.

Using the $\Omega_t(t = 2, 4, 6)$ parameters, the spontaneous emission probabilites for electric dipole transitions from the J' manifold $|(S', L')\, J'\rangle$ to the termianl manifold $|(S, L)\, J\rangle$ can be calculated by using the equation as shown in Ref. [14].

All the center wavelength λ_p, total spontaneous emission probilities A_{total}, branching ratios β, and radiative lifetimes τ_{rad} of Nd^{3+}: $^4F_{3/2} \rightarrow {}^4I_{15/2}$, $^4I_{13/2}$, $^4I_{11/2}$, and $^4I_{9/2}$ transitions were calculated and listed in Table 1. The high values of the A_{total} compared with other oxide host are mainly due to the high refractive index ($\geq$ 2.0) of tellurite glass.

The peak stimulated emission cross sections $\sigma\ (J, J')$ were determined by[11]

$$\sigma\,(J;J') = \frac{\lambda_p^4}{8\pi c n^2 \Delta\lambda_{\text{eff}}} A_{\text{rad}}[(^4F_{3/2}; {}^4I_J)], \qquad (1)$$

where A_{rad} is the spontaneous emission probability, n is the refractive index, c is the velocity of light, and $\Delta\lambda_{\text{eff}}$ is the fluorescence effective linewidth which was expressed by

$$\Delta\lambda_{\text{eff}} = \frac{\int I(\lambda)\mathrm{d}\lambda}{I_{\text{p}}}, \qquad (2)$$

where $I(\lambda)$ is the intensity of at the wavelength λ, I_{p} is the intensity at the peak wavelength λ_{p}. Table 2 shows the peak wavelength, the peak stimulated emissions cross section, and the effective fluorescence linewidth of

Table 1. λ_{p}, A_{total}, β, and τ_{rad} of Nd^{3+}: $^4F_{3/2} \rightarrow {}^4I_{15/2}$, $^4I_{13/2}$, $^4I_{11/2}$, and $^4I_{9/2}$ transitions

Transition	λ_{p} (cm^{-1})	A_{total} (s^{-1})	β	τ_{rad} (μs)
$^4F_{3/2} \rightarrow {}^4I_{15/2}$	5324	20	0.003	151
$^4F_{3/2} \rightarrow {}^4I_{13/2}$	7473	517	0.078	
$^4F_{3/2} \rightarrow {}^4I_{11/2}$	9416	3384	0.511	
$^4F_{3/2} \rightarrow {}^4I_{9/2}$	11274	2702	0.408	

Table 2. Spectroscopic properties of Nd^{3+}-doped tellurite bulk glass

	λ_{p} (nm)	σ_{p} (10^{-20} cm^2)	$\Delta\lambda_{\text{eff}}$ (nm)	τ_0 (μs)
$^4F_{3/2} \rightarrow {}^4I_{13/2}$	1338	1.7	57.0	
$^4F_{3/2} \rightarrow {}^4I_{11/2}$	1062	5.0	31.5	
$^4F_{3/2}$ Level Lifetime				164

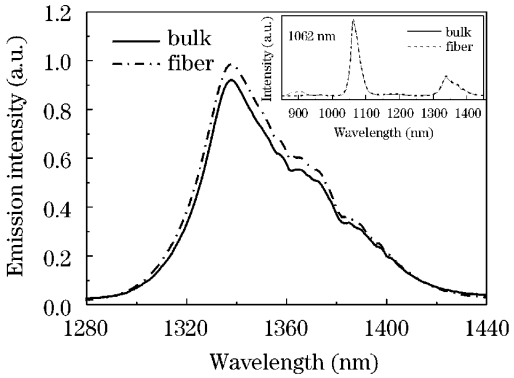

Fig. 3. Comparison of the fluorescence spectra of Nd^{3+}-doped tellurite glass and fiber.

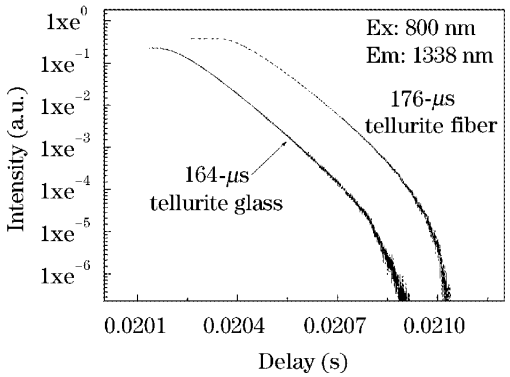

Fig. 4. Fluorescence decay profile of Nd^{3+}: 1338 nm in tellurite glass and fiber.

$^4F_{3/2} \rightarrow {}^4I_{13/2}$ and $^4I_{11/2}$ transitions, and measured lifetime of $^4F_{3/2}$ level in bulk glass. The emssion cross section at 1338 nm in tellurite host is the largest sample among oxide glasses[12], which we suggest that Nd^{3+}-doped tellurite glass could be utilized as rare earths containing devices.

Figure 3 gives the fluorescence spectra of Nd^{3+}-doped tellurite glass and fiber under 800-nm excitation. The emission band centered at 1338 nm is attributed to the transition $^4F_{3/2} \rightarrow {}^4I_{13/2}$. In the case of the bulk glass, the full width at half maximum (FWHM) of bandwidth is about 50 nm, while 55 nm for fiber. The general feature of emission spectra for fiber in Fig. 3 is similar to that observed for bulk. However, the reabsorption with the confinement affects the high energy side (sharp peak) of the resonant transition to the ground level in the fiber with respect to the glass. As can be also seen in the case of glass and fiber, the relative intensity of the $^4F_{3/2} \rightarrow {}^4I_{13/2}$ transition is approximately four times smaller than that of $^4F_{3/2} \rightarrow {}^4I_{11/2}$ transition. Meanwhile, it is necessary to point out that the 1.3-μm

amplifying transition of Nd^{3+} suffers from the competition with amplified spontaneous emission (ASE) at 1.06 μm[3,4], and therefore reduces the amplifier efficiency.

Figure 4 shows luminescence decays corresponding to transitions from the $^4F_{3/2}$ level to the $^4I_{13/2}$ levels, in the tellurite glass and fiber, respectively. The fluorescence intensity I versus the time t was approximated numerically by the following function

$$I = I_0 \exp\left(-\frac{t}{\tau}\right), \tag{3}$$

where I_0 is the initial intensity and τ is the fluorescence decay time. An exponential decay, with $\tau = 176$ μs, was obtained for the fiber. The phonon energy in the proposed tellurite glass is about 750 cm^{-1}, and energy gap of from the $^4F_{3/2}$ level to the next lowest $^4I_{15/2}$ energy level is $\sim$ 5300 cm^{-1}, thus the nonradiative relaxation from $^4F_{3/2}$ level to the lower levels is expected to be negligibly small. From the Tables 1 and 2, whatever in glass or fiber, we see that $\tau_{rad} \leq \tau_0$, the differences being $\approx$ 10%−15%. The quantum efficiency η of the luminescence from the $^4F_{3/2}$ level is determined from $\eta = \tau_0/\tau_{rad}$. Therefore, a quantum efficiency $\eta \approx 1$ for the metastable $^4I_{13/2}$ level both in the glass and fiber.

From above data, the figure-of-merit for gain ($\sigma_p\tau_0$) is the order of 1.7×10^{-20} $cm^2\times164$ μs $\approx$ 2.8×10^{-24} cm^2s, which is quite comparable with the value recently reported for Nd^{3+}- doped fluoroaluminate glasses[3] developed for the 1.3-μm amplifier, and is an order of magnitude larger than Pr^{3+}-doped lead/indium (Pb/In) and indium/gallium (In/Ga) based fluoride glasses[1,2] at approximately 0.3×10^{-24} cm^2s.

In conclusion, The J-O parameters, Ω_t (t = 2, 4, 6), were determined by fitting the experimental oscillator strength due to $4f^3 \rightarrow 4f^3$ transition to J-O theory for electric dipole interaction. The emission from the $^4F_{3/2} \rightarrow {}^4I_{13/2}$ transition of Nd^{3+} in tellurite fiber is at 1.33-μm wavelength with a spectral bandwidth of 55 nm, which is similar to that in bulk glass. The lifetime of $^4F_{3/2}$ level is 164 μs, and the quantum efficiency is ~100%. The figure-of-merit for gain ($\sigma_p\tau_0$) for Nd^{3+}-doped tellurite glass is about 2.8×10^{-24} cm^2s, which is quite comparable with that in Nd^{3+}-doped fluoroaluminate glasses, and is an order of magnitude larger than Pr^{3+}-doped fluoride glasses. Based on the results above, it appears that Nd^{3+}-doped tellurite fiber is promising materials for planer waveguide lasers and amplifiers operating in the 1.3-μm window.

This work was supported by the Rising-Star Project (No. 04QMX1448) of Shanghai Municipal Science and Technology Commission and the National Natural Science Foundation of China (No. 60207006) J. Zhang's e-mail address is zjj@laserglass.com.cn.

References

1. Y. Nishida, T. Kanamori, Y. Ohishi, M. Yamada, K. Kobayashi, and S. Sudo, IEEE Photon. Technol. Lett. **9,** 318 (1997).
2. K. Isshiki, M. Kubota, Y. Kuze, S. Yamaguchi, H. Watanabe, and K. Kasahara, IEEE Photon. Technol. Lett. **10,** 1112 (1998).
3. M. Naftaly and A. Jha, J. Appl. Phys. **87,** 2098 (2000).
4. S. Zemon, B. Pedersen, W. Jminiscalco, B. T. Hall, R. C. Folweiler, B. A. Thompson, and L. K. J. Andrews, IEEE Photon. Technol. Lett. **4,** 244 (1992).
5. E. Ishikawa, H. Aoki, Yamashita, and Y. Asahara, Electron. Lett. **28,** 1497 (1992).
6. M. J. Weber, J. Non-Cryst. Solids. **123,** 208 (1990).
7. J. S. Wang, E. M. Vogel, and E. Snitzer, Opt. Mater. **3,** 187 (1994).
8. A. Mori, Y. Ohishi, and S. Sudo, Electron. Lett. **33,** 863 (1997).
9. H. Ono, A. Mori, K. Shikano, and M. Shimizu, IEEE Photon. Technol. Lett. **14,** 1070 (2000).
10. J. S. Wang, D. P. Machewirch, F. Wu, E. M. Vogel, and E. Snitzer, Opt. Lett. **19,** 1448 (1994).
11. M. J. Weber, J. D. Myers, and D. H. Blackburn, J. Appl. Phys. **52,** 2944 (1981).
12. J. M. Pellegrino, W. M. Yen, and M. J. Weber, J. Appl. Phys. **51,** 6332 (1980).
13. B. Judd, Phys. Rev. **127,** 750 (1962).
14. G. Ofelt, J. Chem. Phys. **37,** 511 (1962).